

Examination of Microphysical Relationships and Corresponding Microphysical Processes in Warm Fogs

LU Chunsong^{1,2,3*} (陆春松), LIU Yangang³ (刘延刚), NIU Shengjie¹ (牛生杰), ZHAO Lijuan⁴ (赵丽娟),

YU Huaying¹ (于华英) and CHENG Muning⁵ (程穆宁)

¹ Key Laboratory for Aerosol-Cloud-Precipitation of China Meteorological Administration, Collaborative Innovation Center on Forecast and Evaluation of Meteorological Disasters, Nanjing University of Information Science and Technology, Nanjing 210044, China

² State Key Laboratory of Severe Weather, Chinese Academy of Meteorological Sciences, Beijing 100081, China

³ Atmospheric Sciences Division, Brookhaven National Laboratory, NY 11973, US

⁴ Xiamen Environmental Monitoring Central Station, Xiamen 361004, China

⁵ Second Institute of Environmental Assessment, Jiangsu Provincial Academy of Environmental Science, Nanjing 210000, China

(Received July 30, 2013; in final form September 4, 2013)

ABSTRACT

In this paper, the microphysical relationships of 8 dense fog events collected from a comprehensive fog observation campaign carried out at Pancheng (32.2°N, 118.7°E) in the Nanjing area, China in the winter of 2007 are investigated. Positive correlations are found among key microphysical properties (cloud droplet number concentration, droplet size, spectral standard deviation, and liquid water content) in each case, suggesting that the dominant processes in these fog events are likely droplet nucleation with subsequent condensational growth and/or droplet deactivation via complete evaporation of some droplets. The abrupt broadening of the fog droplet spectra indicates the occurrence of the collision-coalescence processes as well, although not dominating. The combined effects of the dominant processes and collision-coalescence on microphysical relationships are further analyzed by dividing the dataset according to visibility or autoconversion threshold in each case. The result shows that the specific relationships of number concentration to volume-mean radius and spectral standard deviation depend on the competition between the compensation of small droplets due to nucleation-condensation and the loss of small droplets due to collision-coalescence. Generally, positive correlations are found for different visibility or autoconversion threshold ranges in most cases, although negative correlations sometimes appear with lower visibility or larger autoconversion threshold. Therefore, the compensation of small droplets is generally stronger than the loss, which is likely related to the sufficient fog condensation nuclei in this polluted area.

Key words: fog microphysics, microphysical relationships, physical processes, observations

Citation: Lu Chunsong, Liu Yangang, Niu Shengjie, et al., 2013: Examination of microphysical relationships and corresponding microphysical processes in warm fogs. *Acta Meteor. Sinica*, **27**(6), 832–848, doi: 10.1007/s13351-013-0610-0.

Supported by National Natural Science Foundation of China (41305120, 41030962, 41275151, 41375138, 41375137, and 41305034), Natural Science Foundation of Jiangsu Province (BK20130988, SK201220841), Specialized Research Fund for the Doctoral Program of Higher Education (20133228120002), China Meteorological Administration Special Public Welfare Research Fund (GYHY201406007), Natural Science Foundation of the Higher Education Institutions of Jiangsu Province (13KJB170014), Open Funding from Key Laboratory for Aerosol-Cloud-Precipitation of China Meteorological Administration (KDW1201, KDW1102), Open Funding from Key Laboratory of Meteorological Disaster of Ministry of Education (KLME1205, KLME1107), Open Funding from State Key Laboratory of Severe Weather (2013LASW-B06), Qing-Lan Project for Cloud-Fog-Precipitation-Aerosol Study in Jiangsu Province, Project Funded by the Priority Academic Program Development of Jiangsu Higher Education Institutions, and U.S. Department of Energy's (DOE) Earth System Modeling (ESM) program via the FASTER project (www.bnl.gov/faster) and Atmospheric System Research (ASR) program.

*Corresponding author: luchunsong110@163.com.

1. Introduction

Fog is a severe environmental hazard that greatly influences traffic, human health, and agricultural products, resulting in heavy economic losses (Gultepe et al., 2007; Tardif and Rasmussen, 2007; Haeffelin et al., 2010; Niu et al., 2010a; Zhang, 2012). To reduce the losses, accurate fog forecast is necessary, and numerical forecast/simulation of fog events has attracted great efforts among researchers (Kong, 2002; Fu et al., 2006, 2008; Bergot et al., 2007; Gao et al., 2007; Roquelaure and Bergot, 2008; Rémy and Bergot, 2010; Shi et al., 2010, 2012; Yang et al., 2010; Zhou and Du, 2010; Kim, 2011; Porson et al., 2011; Jia and Guo, 2012; Li et al., 2012; Stolaki et al., 2012; Thoma et al., 2012; Zhou et al., 2012). Whether the numerical forecast is accurate or not depends greatly on the parameterization of complicated physical processes in fog events (Croft et al., 1997; Li et al., 1997; Gultepe et al., 2007). To explore the macro and micro physical processes, it is important to detect fog/cloud microphysical properties because different macro and micro processes affect fog/cloud size distributions and hence key microphysical properties (Li et al., 1994, 1999; Liu et al., 2008). Furthermore, microphysical properties affect visibility, an important factor in fog forecast. Many researchers related visibility to liquid water content (LWC) (e.g., Eldridge, 1971; Tomasi and Tampieri, 1976; Pinnick et al., 1978; Kunkel, 1984; Bergot and Guedalia, 1994; Stoelinga and Warner, 1999); more recently, Gultepe et al. (2006) extended the parameterization and related visibility to both LWC and droplet number concentration (N). Achtemeier (2008) also discussed the relationship of visibility to fog microphysics. Therefore, studying of fog microphysics is necessary and important to improvement of fog forecast and reduction of losses due to fog disasters.

In the past several decades, great efforts have been devoted to in situ observational studies on fog microphysics (Pilié et al., 1975; Roach et al., 1976; Meyer et al., 1986; Gerber, 1991; Fuzzi et al., 1992; Wendisch et al., 1998; Gultepe et al., 2006; Lu and Niu, 2008; Haeffelin et al., 2010; Niu et al., 2010c; Price, 2011; Yue et al., 2012, 2013; Zhang et al., 2013). In most

fog cases, LWC is lower than 0.5 g m^{-3} (e.g., Wobrock et al., 1992; Niu et al., 2010b); N is from a few tens to several hundreds per cubic centimetre (García-García and Montañez, 1991; Klemm and Wrzesinsky, 2007; Gultepe et al., 2009; Liu et al., 2011; Zhao et al., 2013; Zhou et al., 2013), but N larger than 1000 cm^{-3} is also found in some polluted areas (Li, 2001; He et al., 2003; Niu et al., 2010b); both unimodal (García-García and Montañez, 1991; Li, 2001; Niu et al., 2010c; Gonser et al., 2012) and bimodal (Hong and Huang, 1965; Pilié et al., 1975; Roach et al., 1976; Meyer et al., 1980; Gerber, 1991; Wendisch et al., 1998; Huang et al., 2000; Gultepe et al., 2009; Niu et al., 2012) size distributions have been observed in different fog cases. Furthermore, during individual fog events, remarkable spatial and temporal variations of microphysical properties have been widely reported. Spatially, similar to inhomogeneity in clouds (e.g., Baumgardner et al., 1993; Burnet and Brenguier, 2007; Haman et al., 2007), García-García et al. (2002) found inhomogeneous fog microphysical structures on a fine scale (less than 1 m). Temporally, in addition to evident lifecycle variation, quasi-periodic oscillations of the microphysical properties and other related meteorological elements (e.g., temperature and wind speed) have been observed and simulated; different mechanisms for the quasi-periodic oscillations were proposed by different scholars, such as a cycle of fog dissipation and redevelopment processes associated with radiative cooling and turbulence (Welch et al., 1986), interaction between radiation-induced droplet growth and subsequent depletion of droplets due to gravitational settling (Bott et al., 1990; Huang et al., 2000), advection of fog inhomogeneous spatial structure (Roach et al., 1976), and effect of gravity wave (Roach, 1976; Duynkerke, 1991). Fog droplet size distributions also have significant variability due to the effects of different processes, such as activation, diffusional growth of droplets, turbulent mixing, gravitational settling (Niu et al., 2010b), etc. For example, explosive broadening of droplet size distributions have been found in observations (Pu et al., 2008; Lu et al., 2010a; Niu et al., 2012), which is directly related to microphysical processes, and is further related to macro conditions, such as cooling due to invasion of

weak cold air, cooling due to long wave radiation, and water vapor advection.

Although the importance of fog microphysics and related processes has been recognized and considerable progress has been made, much remains elusive. For example, it is still unclear what processes are the main processes in determining fog droplet size distributions. To fill this gap, 8 fog events observed at Pancheng ($32^{\circ}12'N$, $118^{\circ}42'E$), Nanjing, China in 2007 are studied to examine the microphysical relationships and main and minor physical processes. The results will be helpful to improve theoretical understanding of fog physics and parameterization of fog/cloud physics in models.

In addition, past fog observations in China were largely based on gelatin-slide impactor systems with a low sampling rate (Niu et al., 2010b). A droplet spectrometer (FM-100; Droplet Measurement Technologies, Colorado, USA) with a sampling rate of 1 Hz was deployed at Pancheng in 2007. The data collection from this spectrometer provides a great opportunity to examine fog microphysics and the corresponding physical processes. Furthermore, Nanjing is a megacity in the Yangtze River Delta of China with high population density and a well-developed economy; urbanization has brought great stress to the local environment and emissions of pollutants (SO_2 , NO_x , and NH_3) are one or two orders of magnitude higher than in Europe and South America (Lu et al., 2010b). Fog occurring in such a polluted environment is expected to show unique microphysical characteristics, compared with fogs in clean areas.

The rest of the paper is organized as follows. Section 2 briefly describes the observation site, the key instruments, and the data. Section 3 presents the main results, including the general features of key microphysical properties and their mutual relationships under different conditions, and the discussion on the main and minor microphysical processes. Concluding remarks are presented in Section 4.

2. Observation site and data

The sampling site is located at Pancheng ($32^{\circ}12'N$, $118^{\circ}42'E$; 22 m above sea level) in Nanjing.

This area is unique from several perspectives (Fig. 1). It is located to the north of the Yangtze River and adjacent to the Jiajiang River, which is a tributary of the Yangtze River. Furthermore, it is close to heavy pollution sources such as petrochemical factories, a steel plant, a thermal power station, a nitrogenous fertilizer plant, and highways. Further details can be found in Lu et al. (2010b). The data used in this study were collected from 15 November through 29 December 2007.

Similar to the observations at the same site in 2006 (Liu et al., 2010; Niu et al., 2010c), visibility was automatically measured and recorded every 15 s by a visibility meter (ZQZ-DN; the Radio Scientific Research Institute, Wuxi, Jiangsu, China); surface meteorological quantities (surface air temperature, relative humidity, wind speed, and wind direction) were observed with an automatic weather station (EnviroStationTM, ICT International Pty Ltd, Armidale, New South Wales, Australia); the size distributions of fog droplets were measured with a droplet spectrometer (FM-100) (Eugster et al., 2006; Gultepe et al., 2009). It measures fog droplets of $0.5\text{--}25\ \mu\text{m}$ in radius at a sampling rate of 1 Hz, but the data from the bin $0.5\text{--}1.0\ \mu\text{m}$ are thought to be noisy, which are not included in the calculations of microphysical properties such as N , volume-mean radius (r_v), standard deviation (σ), and LWC. The dataset is averaged to 1 min for this study.

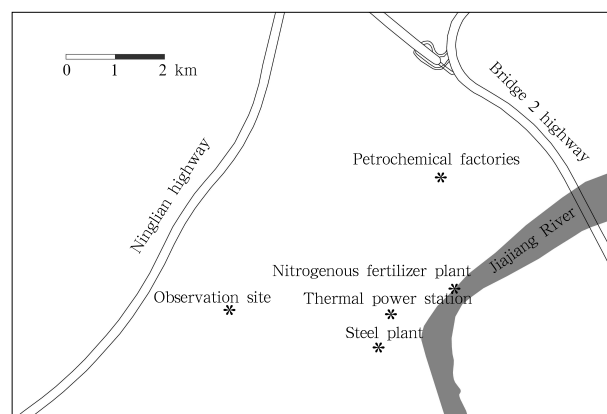


Fig. 1. Map of the observation site Pancheng and its vicinity.

3. Results

3.1 General microphysical characteristics

A total of 8 typical dense fog episodes were observed during the campaign in 2007. The eight cases shared some common features of synoptic weather background. At 500 hPa, Nanjing was often located at the front of an aerological weak trough or in straight northwest wind. At mid and low levels, Nanjing was often controlled by local vortex shear and southwesterly wind. On the surface maps, Nanjing was basically in a uniform-pressure region in front of a high pressure system or influenced by a high pressure system moving into the sea. Table 1 shows the duration, the surface air temperature, and the microphysical properties in these cases. The durations of these cases are in the range of 4.3–25.3 h, and all the cases except case 7 have severe fog periods which are defined in light of visibility (vis) < 50 m (China Meteorological Administration, 2007). According to the review of fog research by Gultepe et al. (2007), Petterssen (1956) suggested that fog can be divided into three subsections: liquid fog (temperature $\geq -10^\circ\text{C}$), mixed phase fog ($-30^\circ\text{C} \leq$ temperature < -10°C), and ice fog (temperature < -30°C); it follows that the events observed in our

experiments are all liquid fogs with average temperature above 0°C .

In each case, N , LWC, r_v , and σ have large standard deviations due to both the spatial inhomogeneous structure (García-García et al., 2002) of the fog and the temporal evolution at different stages in each fog event. Peak radius (r_p) is unique, always at $1.4 \mu\text{m}$; this peak is not a real peak because it is at the first bin, but we still call it “peak” for convenience; similar spectral shape (peak at $1.4 \mu\text{m}$) was also observed by García-García and Montañez (1991) and Gonser et al. (2012); more discussion about the formation of the peak will be given later. Because of the peak at the first bin, the average values of r_v are smaller than the results observed in Sierra Madre Oriental, Mexico (García-García and Montañez, 1991) and in Pico del Este, Puerto Rico (Eugster et al., 2006). Although the average N is generally comparable with the results reported by Gultepe et al. (2009), the maximum N (around 800 cm^{-3}) is much higher, caused by the high pollution level at this site (Lu et al., 2010b; Yang et al., 2012). Generally, the average LWC is comparable with that in the fogs in Pico del Este, Puerto Rico (Eugster et al., 2006) and Fichtelgebirge, Germany (Thalmann et al., 2002). Compared with the fog at the same

Table 1. The duration, surface air temperature, and key microphysical properties in the eight fog cases

Case	Formation time (LST)	Dissipation time (LST)	Duration (h)	Duration of visibility < 50 m (h)	Temperature ($^\circ\text{C}$)	Concentration N (cm^{-3})	Liquid water content LWC (g m^{-3})	Volume -mean radius r_v (μm)	Maximum r_v (μm)	Spectral standard deviation σ (μm)	Peak radius r_p (μm)
1	12/10/2007 22:31	12/11/2007 12:30	14.0	2.0	3.8 (1.4)	64.2 (139.9)	0.022 (0.061)	2.4 (0.9)	5.3	0.9 (0.6)	1.4 (0)
2	12/13/2007 21:55	12/14/2007 11:20	13.5	4.3	0.6 (1.2)	172.6 (248.0)	0.074 (0.127)	2.6 (1.5)	6.1	1.0 (1.0)	1.4 (0)
3	12/14/2007 20:48	12/15/2007 12:02	15.2	0.8	2.2 (1.7)	21.6 (71.3)	0.001 (0.004)	2.0 (0.2)	3.6	0.7 (0.2)	1.4 (0)
4	12/18/2007 02:28	12/18/2007 11:11	8.7	1.8	4.0 (0.8)	81.7 (127.5)	0.021 (0.046)	2.3 (1.0)	5.2	0.8 (0.7)	1.4 (0)
5	12/18/2007 16:07	12/19/2007 12:28	20.4	6.5	3.8 (2.1)	128.9 (185.4)	0.041 (0.084)	2.6 (1.2)	5.9	1.0 (0.8)	1.4 (0)
6	12/19/2007 16:37	12/20/2007 16:11	23.6	13.0	4.6 (1.3)	138.7 (145.5)	0.037 (0.068)	2.8 (1.3)	6.7	1.1 (0.9)	1.4 (0)
7	12/20/2007 17:48	12/21/2007 19:06	25.3	0.0	7.7 (0.7)	39.5 (60.8)	0.003 (0.009)	2.0 (0.4)	3.9	0.6 (0.2)	1.4 (0)
8	12/23/2007 01:16	12/23/2007 05:30	4.3	1.3	5.6 (0.5)	140.5 (127.1)	0.040 (0.048)	3.5 (1.2)	5.8	1.6 (0.8)	1.4 (0)

The figures in the parenthesis are the values of standard deviations of the corresponding properties.

site in 2006 (Niu et al., 2010c), the cases in this study have the same r_p , smaller N , LWC, r_v , and σ . It is noteworthy that the same droplet spectrometer (FM-100) was used in the above observations, except the observation in Sierra Madre Oriental, Mexico, where Forward Scattering Spectrometer Probe (FSSP) (García-García and Montañez, 1991) was used; however, FSSP is similar to FM-100. The similar or same instruments assure more reliable comparisons.

3.2 The dominant microphysical processes

As mentioned above, fog/cloud droplet size distributions and hence the key microphysical properties (N , LWC, r_v , and σ) are determined by different physical mechanisms; different relationships among these microphysical properties are expected in response to different physical mechanisms (Liu et al., 2008; Liu et al., 2011). Therefore, to examine the physical mechanisms, microphysical relationships among N , LWC, r_v , and σ are analyzed. Table 2 shows that these relationships are all positive in the 8 cases. Figure 2 shows case 6 as an example. The reason for choosing case 6 is that generally speaking, the values of microphysical properties (Table 1) and correlation coefficients (Table 2) for this case are in the middle of the 8 cases. The positive correlation between r_v and N is opposite to some previous fog observations (e.g., Huang et al., 2000; Niu et al., 2010b; Li et al., 2011) or cloud observations (e.g., Wang et al., 2009). Collision-coalescence is not likely to be responsible for such a phenomenon, because if dominantly affected by collision-coalescence, droplet size (e.g., r_v) would be expected to be negatively correlated with N . The dominant processes seem to be droplet activation with subsequent condensational growth and/or droplet deactivation via some complete droplet evaporation. Similar conclusion was

also drawn in the fog case in 2006 (Niu et al., 2010c). In addition, the fog in situ observation at Wuqing (39°24'N, 117°03'E) between Beijing and Tianjin in China, also shows positive correlations between liquid water content, droplet number concentration, and droplet size in three polluted fog cases (Quan et al., 2011).

To further discern the factors affecting microphysical relationships, the dataset is divided into two groups for each case based on visibility: mature stage ($0 \text{ m} < \text{vis} \leq 500 \text{ m}$) and formation stage ($500 \text{ m} < \text{vis} < 1000 \text{ m}$). In the mature stage in each case, the relationships among the key microphysical properties are all positive; whereas in the formation stage, the relationships are complicated: r_v vs. N and σ vs. N are negatively correlated, and σ vs. r_v and LWC vs. N are positively correlated in each case; the relationships of σ vs. LWC and LWC vs. r_v are different from case to case, negatively, positively, or not correlated. As an example, Fig. 2 shows the microphysical relationships for these two visibility groups in case 6. Compared with that in the mature stages and in the whole fog dataset (Table 2), the different behaviors of microphysical relationships in the formation stages are likely related to the low and almost constant LWC. The LWC is a measure of available water vapor in air, which can be condensed into liquid water under certain environmental conditions, such as appropriate water vapor mixing ratio, air temperature, and air pressure. In the 8 cases, temperature gradually decreases and relative humidity is 100% at the formation stage with $500 \text{ m} < \text{vis} < 1000 \text{ m}$; fog forms but LWC increases slowly, close to 0. The competition for the limited LWC is expected to be remarkable because fog condensation nuclei are considered as sufficient due to the pollutant emission from the nearby industrial park (Lu

Table 2. Correlation coefficients of the relationships among the key microphysical properties of the eight fog cases

Case	r_v-N	$\sigma-N$	$\sigma-r_v$	$\sigma-LWC$	LWC- N	LWC- r_v
1	0.83	0.82	1.00	0.85	0.93	0.86
2	0.90	0.89	1.00	0.93	0.88	0.94
3	0.27	0.19	0.98	0.23	0.96	0.31
4	0.87	0.86	1.00	0.91	0.87	0.91
5	0.83	0.81	1.00	0.82	0.83	0.83
6	0.71	0.70	1.00	0.78	0.70	0.79
7	0.69	0.65	0.99	0.71	0.86	0.74
8	0.34	0.33	1.00	0.72	0.64	0.73

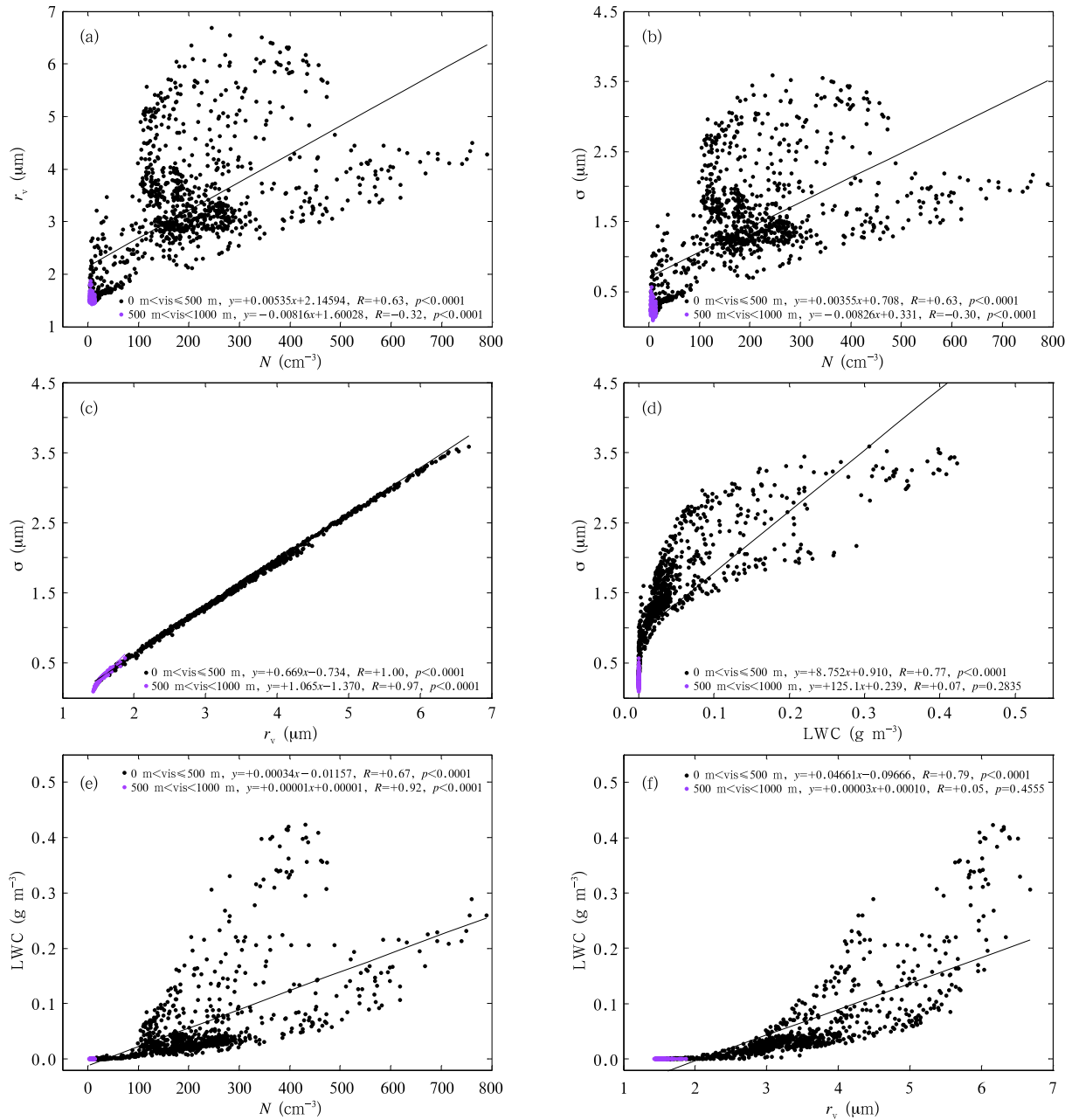


Fig. 2. Relationships (a) between the volume-mean radius (r_v) and the droplet number concentration (N), (b) between the standard deviation (σ) and N , (c) between σ and r_v , (d) between σ and LWC, (e) between LWC and N , and (f) between LWC and r_v , for two visibility (vis) ranges in case 6.

et al., 2010b) and the high water-soluble fraction of aerosol in this area (Wang et al., 2002, 2003). As a result, most droplets are small droplets and concentrated in the first bin (Fig. 3), decreasing r_v and σ with an increase in N . The complicated relationship of LWC to other properties is also probably related to the nearly constant LWC. In the mature stages, LWC

is positively correlated to N , σ , and r_v (Fig. 2), indicating that the available water vapor is sufficient and the competition for water vapor is weak. Therefore, LWC is an important factor affecting the effect of the dominant processes, such as droplet activation with subsequent condensational growth and/or droplet deactivation via some complete droplet evaporation, on

microphysical relationships. Zhang et al. (2011) also found that the value of LWC greatly affects the nucleation of aerosol, cloud number concentration, and droplet size.

3.3 The combined effect of the dominant processes and collision-coalescence

The dominance of droplet nucleation with subsequent condensational growth and/or droplet deactivation via some complete droplet evaporation cannot rule out the roles of other mechanisms. Fog explosive development is a frequent phenomenon (Pu et al., 2008; Lu et al., 2010a; Niu et al., 2012) with a sharp decrease in visibility to below 50 m during a short period of time (e.g., 30 min). An example during a period in case 5 is shown in Figs. 4 and 5. The LWC, N , r_v , σ , and maximum radius (r_{\max}) remarkably increase during 0140–0150 local standard time (LST); correspondingly, the size distributions broaden quickly. It is noteworthy that it takes only 4 min to produce the droplets with r_{\max} around 15 μm (at 0144 LST) from the droplets with r_{\max} around 7 μm (at 0140 LST). Similar explosive developments were also observed in previous fog experiments (Wobrock et al., 1992). Furthermore, some r_{\max} values are even larger than 20 μm (Fig. 4f) and Fig. 3 shows that the average size distributions in the mature stage have r_{\max} in the range of 24–25 μm . It is not likely that condensation is the only mechanism responsible for the formation of big droplets because condensational growth rate of droplet size is negatively correlated with the droplet size itself (e.g., Rogers and Yau, 1989) and supersaturation in fog is often low (e.g., Hudson, 1980); collision-coalescence is likely to be important, although not dominating. It is often thought that gravitational collision-coalescence could not proceed until the radius of droplets exceeds 20 μm (e.g., Jonas, 1996; Yum, 1998). The appearance of larger droplets ($> 20 \mu\text{m}$) shows the possibility of the occurrence of gravitational collision-coalescence.

To further explore the effect of gravitational collision-coalescence intensity on the microphysical relationships, autoconversion threshold function (T) proposed by Liu et al. (2005, 2006) is calculated for all

the cases (see the Appendix for details). A larger value of T indicates a stronger collision-coalescence process, ranging from no action ($T = 0$) to full action ($T = 1$). The result shows that 5 out of 8 cases have T values smaller than 0.2, i.e., gravitational collision-coalescence

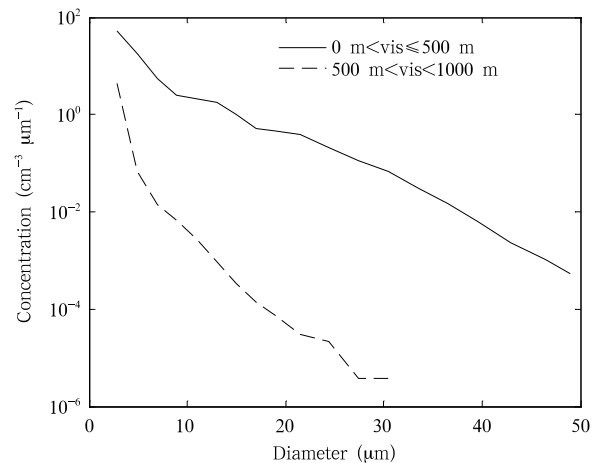


Fig. 3. Average size distributions for two visibility (vis) ranges in case 6.

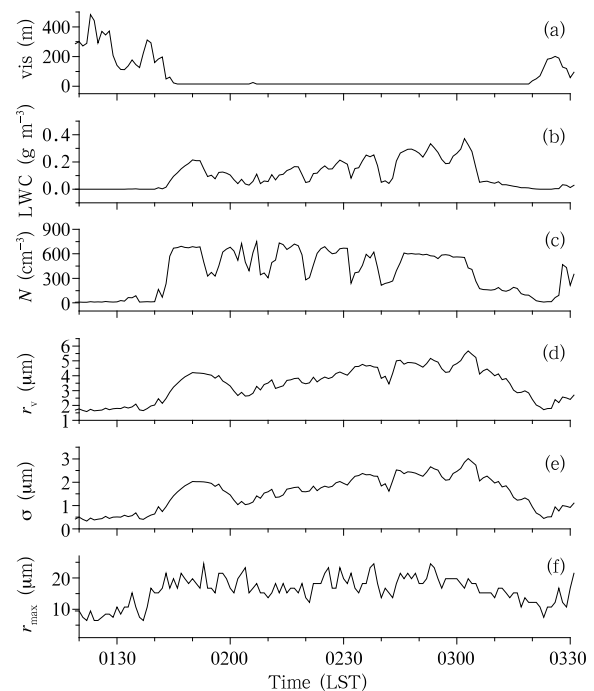


Fig. 4. Temporal evolutions of (a) visibility (vis), (b) liquid water content (LWC), (c) number concentration (N), (d) volume-mean radius (r_v), (e) spectral standard deviation (σ), and (f) maximum radius (r_{\max}) during 0120–0330 LST in case 5.

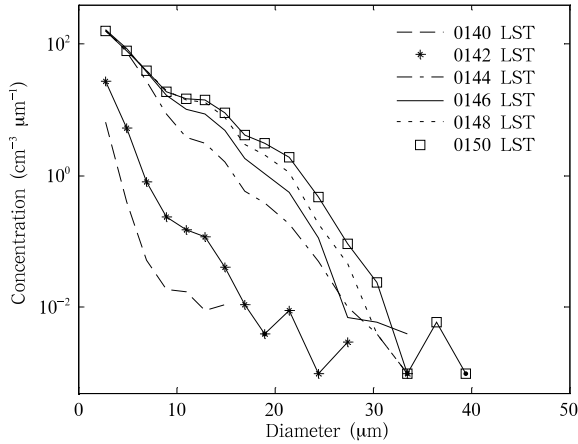


Fig. 5. One minute average size distributions during the fog explosive development in case 5.

nce is weak for most cases; but still, for cases 2, 5, and 6, the maximum values of T are 0.57, 0.47, and 0.80, respectively, showing the importance of gravitational collision-coalescence in the three cases. In addition to gravitational collision-coalescence, Xue et al. (2008) and Ghosh et al. (2005) pointed out that turbulence could significantly enhance the collision rate for cloud droplets ($> 10 \mu\text{m}$ in radius). Therefore, in addition to the dominant mechanisms, the collision-coalescence, especially that enhanced by turbulence, may be important in these fog cases as well.

To address the combined effects of the dominant processes and collision-coalescence in detail, the mature stages ($0 \text{ m} < \text{vis} \leq 500 \text{ m}$) are further divided into three groups based on visibility: 0–50, 50–200, and 200–500 m. Generally, the microphysical relationships are kept positive for the three visibility groups in all the cases except cases 2 and 8. As an example, Fig. 6 shows the relationships for the four visibility groups in case 6. Figure 7 further shows that the size distributions broaden in case 6 with a decrease in visibility. Thus, we assume collision-coalescence becomes more and more vigorous with decreasing visibility. During collision-coalescence, the formation of big droplets consumes small ones, tending to cause increases in r_v and σ , and a decrease in N . However, the relationships of r_v vs. N and σ vs. N are not negative; we argue that this is likely due to the reproduction of small droplets, which can compensate the loss of small

droplets during collision-coalescence and result in synchronous increases in N , r_v , and σ . The reproduction can be caused by the growth of droplets ($< 1 \mu\text{m}$ in radius). As mentioned above, the droplets ($0.5\text{--}1 \mu\text{m}$ in radius) can be measured by the spectrometer, but not included in the calculations of microphysical properties because the data in this bin are thought to be noisy. However, they can still give some hints; the number concentration in this bin is always larger than the value at the current peak at $1.4 \mu\text{m}$ in radius, so it is important that the reproduction of small droplets is through the growth of droplets ($0.5\text{--}1 \mu\text{m}$ in radius). Furthermore, the high concentration of droplets ($0.5\text{--}1 \mu\text{m}$ in radius) always exists, which could be caused by the nucleation of sufficient fog condensation nuclei and subsequent condensation. The positive correlations of LWC to σ , N , and r_v (Figs. 6d, 6e, and 6f) indicate that there is sufficient LWC that could enhance the nucleation of aerosol (Zhang et al., 2011). The reproduction of small droplets confirms the dominant processes identified above and causes the stable peak radius at $1.4 \mu\text{m}$. Therefore, the sufficient fog condensation nuclei in the polluted area, along with the higher LWC, is important for the positive correlations of r_v vs. N and σ vs. N . Similar phenomena were also presented by Hudson and Svensson (1995), they analyzed the cloud microphysical properties off the southern California coast and found that in three cases which had larger cloud condensation nuclei due to the effect of ship exhaust plumes, r_v and N showed positive correlations, whereas for other cases, the correlation was negative. Furthermore, Wang et al. (2009) examined the marine clouds observed off the coast of Monterey and Point Reyes, northern California with data reflecting ship exhaust plumes deleted, and found a negative correlation between r_v and N ; the average size distributions along different flight horizontal levels showed small number concentration of small droplets, indicative of insufficient reproduction of small droplets by nucleation after cloud formation.

However, negative correlations of r_v vs. N and σ vs. N are found for $0 \text{ m} < \text{vis} \leq 50 \text{ m}$ in case 2 (figure omitted) and in case 8 (Fig. 8). In the above discussion, the negative correlations for $500 \text{ m} < \text{vis}$

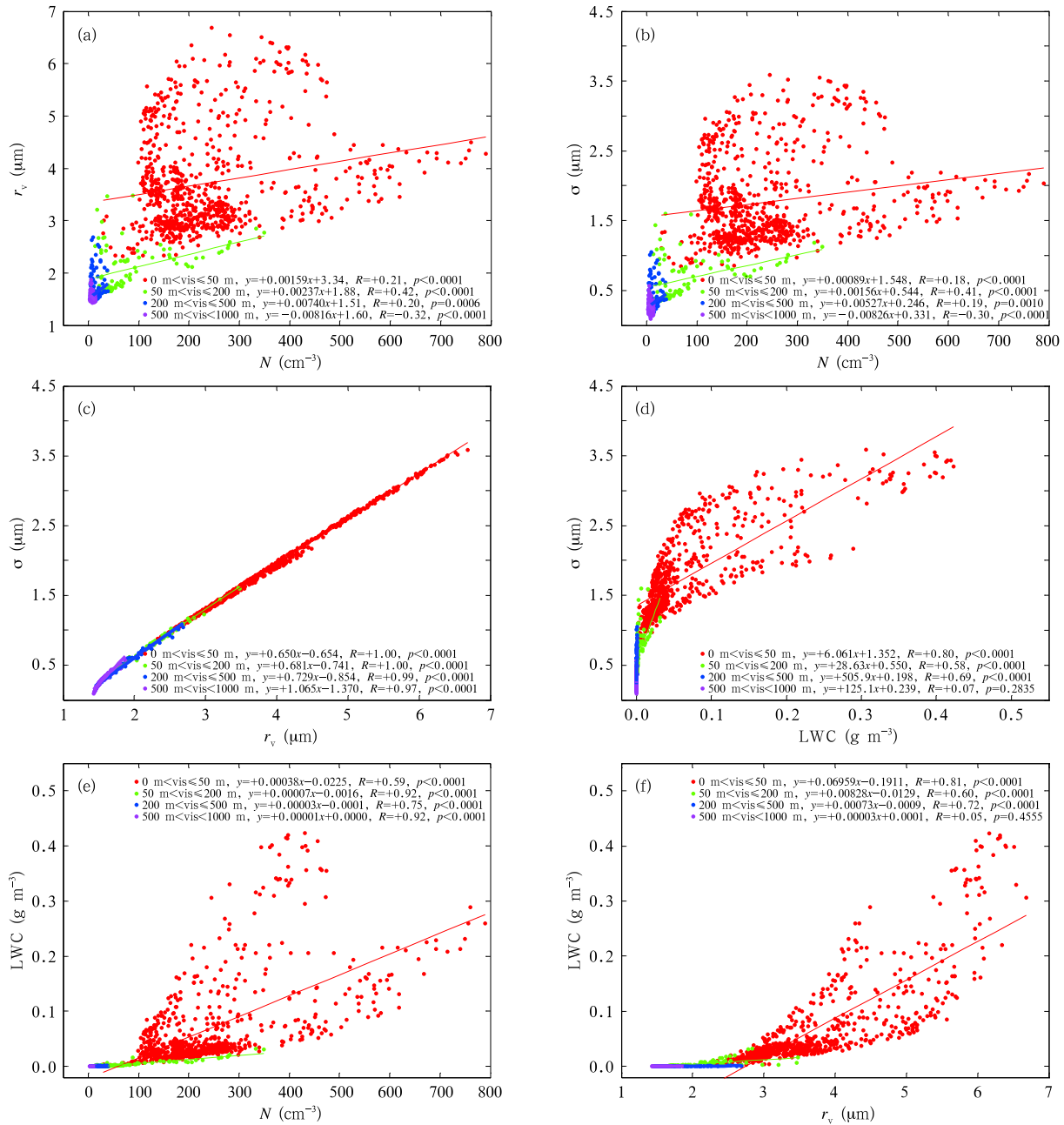


Fig. 6. As in Fig. 2, but for four visibility (vis) ranges in case 6.

< 1000 m are due to the competition for nearly constant LWC and sufficient fog condensation nuclei. But here LWC is not close to a constant as indicated by the positive correlations of σ vs. LWC, LWC vs. N , and LWC vs. r_v (Figs. 8d, 8e, and 8f). Thus, collision-coalescence could be an important reason for the negative correlations. Furthermore, with a decrease in

visibility, the relationships of r_v vs. N and σ vs. N change from positive ($200 \text{ m} < \text{vis} \leq 500 \text{ m}$) to irrelevant ($50 \text{ m} < \text{vis} \leq 200 \text{ m}$), and then to negative correlations ($0 \text{ m} < \text{vis} \leq 50 \text{ m}$). Similar conclusion can be drawn for case 2. In other cases, there is a similar trend. For example, in case 6 (Fig. 6), the slope of r_v vs. N decreases from 0.00740 ($200 \text{ m} < \text{vis} \leq$

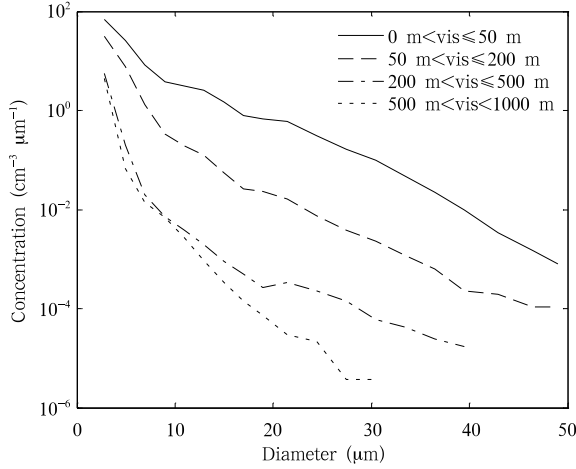


Fig. 7. Average size distributions for four different visibility (*vis*) ranges in case 6.

500 m) to 0.00237 ($50 \text{ m} < \text{vis} \leq 200 \text{ m}$), and then to 0.00159 ($0 \text{ m} < \text{vis} \leq 50 \text{ m}$). Therefore, in all the cases analyzed, the slopes of r_v vs. N and σ vs. N decrease with increasing visibility, consistent with the assumption that collision-coalescence becomes stronger. We argue that whether r_v vs. N and σ vs. N are positively, negatively, or not correlated in all the eight cases depends on the competition between the loss of small droplets due to collision-coalescence and the compensation of small droplets due to nucleation and condensation; generally, compensation is larger than the loss because six cases have positive correlations for lower visibility, and only two cases have negative correlations.

In the above discussion, turbulent and gravitational collision-coalescence processes are assumed to be stronger for a lower visibility. Based on T , the effect of gravitational collision-coalescence can be further studied. The data in cases 2, 5, and 6, which have T larger than 0.2, are divided based on the same T ranges in Niu et al. (2010c) ($0 \leq T \leq 0.2$, $0.2 < T < 0.6$, and $0.6 \leq T \leq 1.0$). Cases 2 and 5 have the first two T ranges. Case 6 has three T ranges but the data points for $0.6 \leq T \leq 1.0$ are rare; so $0.2 < T < 0.6$ and $0.6 \leq T \leq 1.0$ are combined to be $0.2 < T \leq 1.0$ for case 6. Figure 9 shows case 6 as an example. The negative correlations of r_v vs. N and σ vs. N for higher T show that the loss of small droplets due to gravitational collision-coalescence is expected

to be higher than the compensation. Similar phenomena are found in cases 2 and 5. Furthermore, it is interesting to find that r_v vs. N and σ vs. N are negative for $0.2 < T \leq 1.0$ (Figs. 9a and 9b) but positive for $0 \text{ m} < \text{vis} \leq 50 \text{ m}$ (Figs. 6a and 6b) in case 6. Comparison of the two figures indicates that the data points with $0 \text{ m} < \text{vis} \leq 50 \text{ m}$ are much more than those with $0.2 < T \leq 1.0$. Therefore, only a few size distributions are affected by gravitational collision-coalescence; most droplet spectral broadening is likely related to turbulent collision-coalescence. The reproduction of small droplets can compensate the loss of small droplets due to turbulent collision-coalescence but not gravitational collision-coalescence.

It is interesting to find that cases 2, 5, 6, and 8 have negative correlations for a large T or a low visibility. These cases have larger mean LWC, mean r_v , and maximum r_v than the other cases (Table 1). An important reason is that there was precipitation before the fog events and evaporation of water in the soil provided plenty of water vapor.

4. Concluding remarks

Warm fog microphysics is examined using the in situ observations conducted at Pancheng in 2007. Through analysis of the different microphysical relationships in the eight fog cases, the microphysical processes and key factors affecting fog microphysics are explored.

It is shown that the key microphysical properties such as droplet number concentration (N), volume-mean radius (r_v), spectral standard deviation (σ), and liquid water content (LWC) in the eight cases all exhibit positive correlations with one another, indicating that the dominant microphysical process is likely to be droplet activation with subsequent condensational growth and/or droplet deactivation via some complete droplet evaporation. The LWC is a key factor affecting the effect of the dominant processes on microphysical relationships. In the formation stages ($500 \text{ m} < \text{vis} < 1000 \text{ m}$), σ vs. N and r_v vs. N are negatively correlated due to the competition of sufficient fog condensation nuclei for nearly constant LWC; in the mature stages ($0 \text{ m} < \text{vis} \leq 500 \text{ m}$), the LWC is not close to a

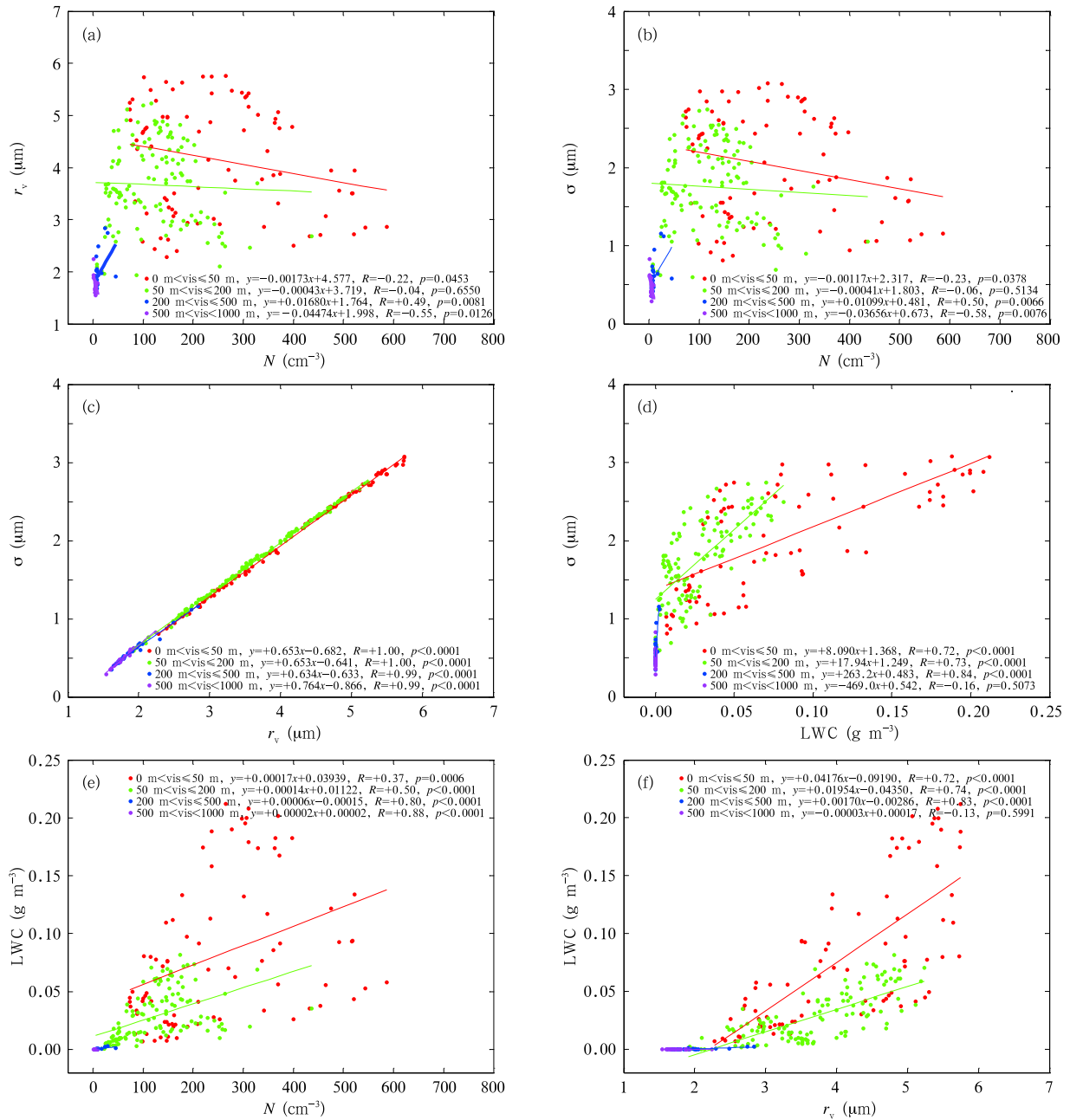


Fig. 8. As in Fig. 6, but for case 8.

constant, but positively correlated to N , σ , and r_v , as a result, the competition for LWC is not remarkable and σ vs. N and r_v vs. N are positively correlated.

Besides the dominant mechanism, the explosive development along with abrupt broadening of fog droplet size distributions indicates that turbulent and gravitational collision-coalescence processes are also important. The mature stages ($0 \text{ m} < \text{vis} \leq 500 \text{ m}$)

are further divided into three groups ($0 \text{ m} < \text{vis} \leq 50 \text{ m}$, $50 \text{ m} < \text{vis} \leq 200 \text{ m}$, and $200 \text{ m} < \text{vis} \leq 500 \text{ m}$). Positive correlations among LWC, N , r_v , and σ hold in the three visibility ranges for six cases; in the other two cases (cases 2 and 8), LWC vs. N , LWC vs. r_v , σ vs. LWC, and σ vs. r_v are positive, but the correlations of r_v vs. N and σ vs. N are found from positive to irrelevant, and to negative correlations with the

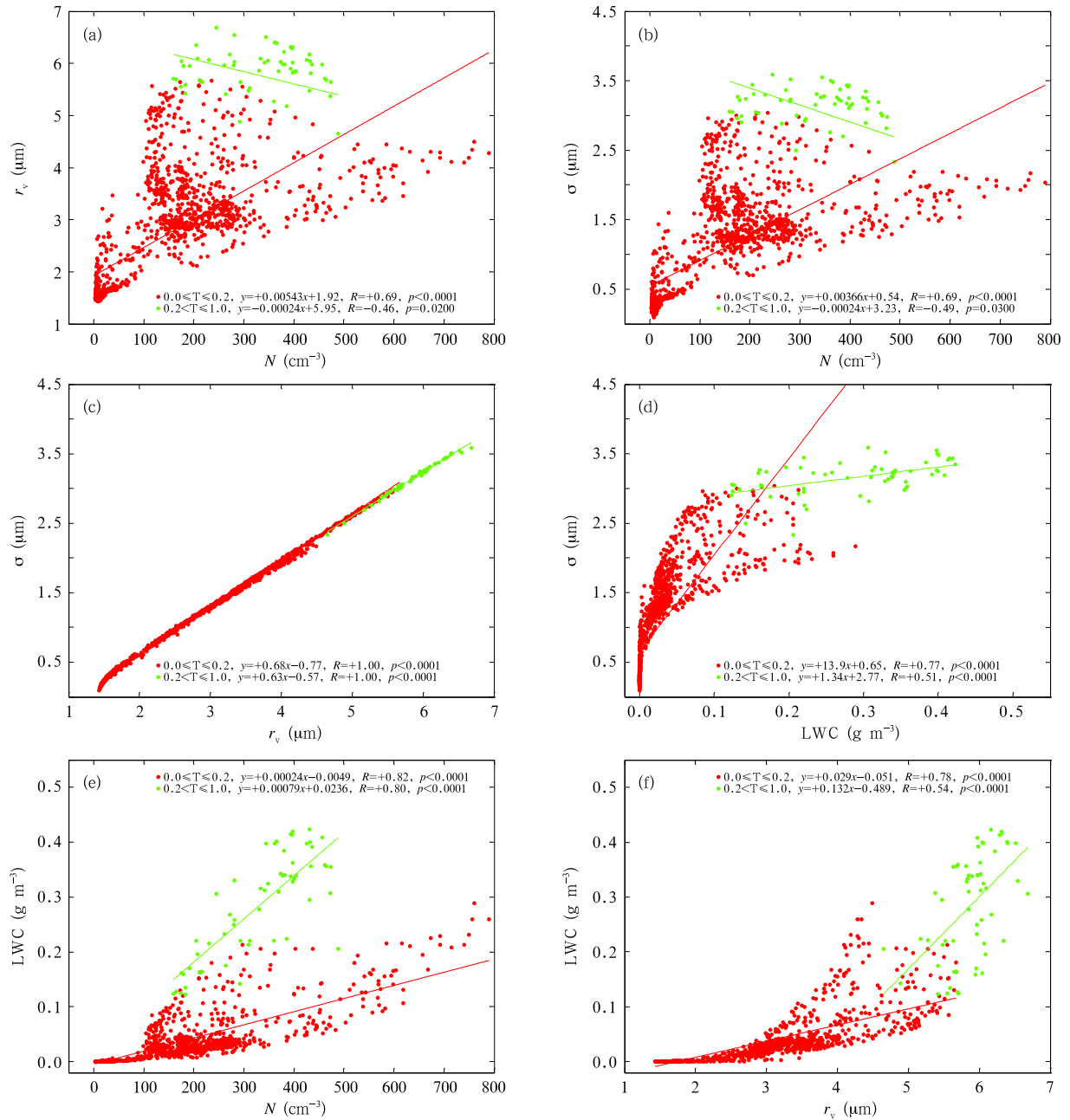


Fig. 9. As in Fig. 2, but for two autoconversion threshold function (T) ranges in case 6.

decreasing visibility, indicating increasingly stronger collision-coalescence. We argue that the complicated relationships of r_v vs. N and σ vs. N are closely related to the competition between the loss of small droplets due to collision-coalescence and the compensation of small droplets due to nucleation and condensation. Generally, the compensation is larger than the

loss because of the large concentration of fog condensation nuclei in this polluted area.

To further explore the effect of gravitational collision-coalescence, autoconversion threshold function (T) is calculated. Among the 8 cases, cases 2, 5, and 6 have T larger than 0.2 and the dataset is divided based on T values. Negative correlations of r_v

vs. N and σ vs. N are found for a large T . Furthermore, with the increasing T , correlation coefficients of σ vs. r_v , σ vs. LWC, LWC vs. N , and LWC vs. r_v become less positive or even negative. The gravitational collision-coalescence tends to weaken the positive correlations among key microphysical properties caused by the dominant processes.

Two points are noteworthy. First, numerical models are also useful to study fog lifecycle and related microphysical processes, but main-stream fog models do not consider the effect of turbulence well, such as turbulent collision-coalescence (e.g., Bergot and Guedalia, 1994; Shi et al., 1996; Hu et al., 2006). Direct numerical simulation is another tool for studying microphysical processes in fogs, especially quantitative description of the influence of turbulence on condensational growth and turbulent collision-coalescence. Second, this study focuses on the fog microphysics; it is known that macro conditions for the fog formation, duration, and dissipation are also important to understanding of the microphysical processes (e.g., Huang et al., 2011). For example, as mentioned above, the LWC is greatly affected by some environmental conditions (such as water vapor mixing ratio, air temperature, and air pressure), which are further related to radiation, turbulence, etc. (Zhou and Ferrier, 2008; Yuan and Huang, 2011). Therefore, detailed analysis on the macro mechanisms responsible for fog formation is necessary in future studies.

Appendix

Autoconversion Threshold Function

According to Liu et al. (2005, 2006), all the autoconversion parameterizations that have been developed so far can be generically written as:

$$P = P_0 T, \quad (\text{A1})$$

where P is the autoconversion rate, P_0 is the rate function describing the conversion rate after the onset of the autoconversion process, and T is the threshold function describing the threshold behavior of the autoconversion process. The size truncation function

employed to quantify the effect of truncating the cloud droplet size distribution on the autoconversion rate can be used as a threshold function to represent the threshold behavior associated with the autoconversion process, providing a physical basis for the threshold function. The expression of T can be generally described by:

$$T = \frac{P}{P_0} = \left[\frac{\int_{r_c}^{\infty} r^6 n(r) dr}{\int_0^{\infty} r^6 n(r) dr} \right] \left[\frac{\int_{r_c}^{\infty} r^3 n(r) dr}{\int_0^{\infty} r^3 n(r) dr} \right], \quad (\text{A2})$$

where r is the droplet radius, $n(r)$ is the cloud/fog droplet size distribution, and r_c is the critical radius for autoconversion. Liu et al. (2004) derived an analytical expression for predicting r_c in the autoconversion parameterization:

$$r_c \approx 4.09 \times 10^{-4} \beta_{\text{con}}^{1/6} \frac{N^{1/6}}{\text{LWC}^{1/3}}, \quad (\text{A3})$$

where $\beta_{\text{con}} = 1.15 \times 10^{23}$ is an empirical coefficient.

REFERENCES

- Achtemeier, G. L., 2008: Effects of moisture released during forest burning on fog formation and implications for visibility. *J. Appl. Meteor. Climatol.*, **47**, 1287–1296.
- Baumgardner, D., B. Baker, and K. Weaver, 1993: A technique for the measurement of cloud structure on centimeter scales. *J. Atmos. Oceanic Technol.*, **10**, 557–565.
- Bergot, T., and D. Guedalia, 1994: Numerical forecasting of radiation fog. Part I: Numerical model and sensitivity tests. *Mon. Wea. Rev.*, **122**, 1218–1230.
- , E. Terradellas, J. Cuxart, et al., 2007: Intercomparison of single-column numerical models for the prediction of radiation fog. *J. Appl. Meteor. Climatol.*, **46**, 504–521.
- Bott, A., U. Sievers, and W. Zdunkowski, 1990: A radiation fog model with a detailed treatment of the interaction between radiative transfer and fog microphysics. *J. Atmos. Sci.*, **47**, 2153–2166.
- Burnet, F., and J. L. Brenguier, 2007: Observational study of the entrainment-mixing process in warm convective clouds. *J. Atmos. Sci.*, **64**, 1995–2011.

- China Meteorological Administration, 2007: Specifications for surface meteorological observation. Part IV: Observation of weather phenomenon. QX/T 48-2007. (in Chinese)
- Croft, P. J., R. L. Pfof, J. M. Medlin, et al., 1997: Fog forecasting for the southern region: A conceptual model approach. *Wea. Forecasting*, **12**, 545–556.
- Duynkerke, P. G., 1991: Observation of a quasi-periodic oscillation due to gravity waves in a shallow radiation fog. *Quart. J. Roy. Meteor. Soc.*, **117**, 1207–1224.
- Eldridge, R. G., 1971: The relationship between visibility and liquid water content in fog. *J. Atmos. Sci.*, **28**, 1183–1186.
- Eugster, W., R. Burkard, F. Holwerda, et al., 2006: Characteristics of fog and fogwater fluxes in a Puerto Rican elfin cloud forest. *Agr. Forest Meteorol.*, **139**, 288–306.
- Fu, G., J. T. Guo, S.-P. Xie, et al., 2006: Analysis and high-resolution modeling of a dense sea fog event over the Yellow Sea. *Atmos. Res.*, **81**, 293–303.
- , —, A. Pendergrass, et al., 2008: An analysis and modeling study of a sea fog event over the Yellow and Bohai seas. *Journal of Ocean University of China*, **7**, 27–34.
- Fuzzi, S., M. C. Facchini, G. Orsi, et al., 1992: The Po Valley fog experiment 1989. *Tellus B*, **44**, 448–468.
- Gao, S. H., H. Lin, B. Shen, et al., 2007: A heavy sea fog event over the Yellow Sea in March 2005: Analysis and numerical modeling. *Adv. Atmos. Sci.*, **24**, 65–81.
- García-García, F., and R. A. Montañez, 1991: Warm fog in eastern Mexico: A case study. *Atmósfera*, **4**, 53–64.
- , U. Virafuentes, and G. Montero-Martínez, 2002: Fine-scale measurements of fog-droplet concentrations: A preliminary assessment. *Atmos. Res.*, **64**, 179–189.
- Gerber, H., 1991: Supersaturation and droplet spectral evolution in fog. *J. Atmos. Sci.*, **48**, 2569–2588.
- Ghosh, S., J. Dávila, J. C. R. Hunt, et al., 2005: How turbulence enhances coalescence of settling particles with applications to rain in clouds. Proceedings of the Royal Society A; Mathematical, Physical and Engineering Sciences, **461**, 3059–3088.
- Gonser, S. G., O. Klemm, F. Griessbaum, et al., 2012: The relation between humidity and liquid water content in fog: An experimental approach. *Pure Appl. Geophys.*, **169**(5–6), 821–833.
- Gultepe, I., M. D. Müller, and Z. Boybeyi, 2006: A new visibility parameterization for warm-fog applications in numerical weather prediction models. *J. Appl. Meteor. Climatol.*, **45**, 1469–1480.
- , R. Tardif, S. C. Michaelides, et al., 2007: Fog research: A review of past achievements and future perspectives. *Pure Appl. Geophys.*, **164**, 1121–1159.
- , B. Hansen, S. G. Cober, et al., 2009: The fog remote sensing and modeling field project. *Bull. Amer. Meteor. Soc.*, **90**, 341–359.
- Haefelin, M., T. Bergot, T. Elias, et al., 2010: PARIS-FOG: Shedding new light on fog physical processes. *Bull. Amer. Meteor. Soc.*, **91**, 767–783.
- Haman, K. E., S. P. Malinowski, M. J. Kurowski, et al., 2007: Small scale mixing processes at the top of a marine stratocumulus—A case study. *Quart. J. Roy. Meteor. Soc.*, **133**, 213–226.
- He Youjiang, Zhu Bin, and Ma Li, 2003: The physical process of Chongqing fog's genesis and dissipation in winter. *J. Nanjing Inst. Meteor.*, **26**, 821–828. (in Chinese)
- Hong Zhongxiang and Huang Meiyuan, 1965: The second maximum and other related characteristics of the southern mountain cloud spectra. *The Study on Microphysics of Cloud/Fog Precipitation in China*, J. Zhao, Ed., Science Press, 18–29. (in Chinese)
- Hu Ruijin, Dong Kehui, and Zhou Faxiu, 2006: Numerical experiments with the advection, turbulence and radiation effects in sea fog formation process. *Adv. Mar. Sci.*, **24**, 156–165. (in Chinese)
- Huang, H. J., H. N. Liu, W. M. Jiang, et al., 2011: Characteristics of the boundary layer structure of sea fog on the coast of southern China. *Adv. Atmos. Sci.*, **28**, 1377–1389.
- Huang Yusheng, Huang Yuren, Li Zihua, et al., 2000: The microphysical structure and evolution of winter fog in Xishuangbanna. *Acta Meteor. Sinica*, **58**, 715–725. (in Chinese)
- Hudson, J. G., 1980: Relationship between fog condensation nuclei and fog microstructure. *J. Atmos. Sci.*, **37**, 1854–1867.
- , and G. Svensson, 1995: Cloud microphysical relationships in California marine stratus. *J. Appl. Meteor.*, **34**, 2655–2666.
- Jia Xingcan and Guo Xueliang, 2012: Impacts of anthropogenic atmospheric pollutant on formation and development of a winter heavy fog event. *Chinese J. Atmos. Sci.*, **36**, 995–1008. (in Chinese)

- Jonas, P. R., 1996: Turbulence and cloud microphysics. *Atmos. Res.*, **40**, 283–306.
- Kim, C. K., 2011: An observational and numerical study of sea fog formation off the west coast of the Korean Peninsula. Ph. D. dissertation, Yonsei University, 200 pp.
- Klemm, O., and T. Wrzesinsky, 2007: Fog deposition fluxes of water and ions to a mountainous site in central Europe. *Tellus B*, **59**, 705–714.
- Kong, F. Y., 2002: An experimental simulation of a coastal fog-stratus case using COAMPS(tm) model. *Atmos. Res.*, **64**, 205–215.
- Kunkel, B. A., 1984: Parameterization of droplet terminal velocity and extinction coefficient in fog models. *J. Climate Appl. Meteor.*, **23**, 34–41.
- Li, P. F., X. Li, C. Y. Yang, et al., 2011: Fog water chemistry in Shanghai. *Atmos. Environ.*, **45**, 4034–4041.
- Li, P. Y., G. Fu, C. G. Lu, et al., 2012: The formation mechanism of a spring sea fog event over the Yellow Sea associated with a low-level jet. *Wea. Forecasting*, **27**, 1538–1553.
- Li Zihua, 2001: Studies of fog in China over the past 40 years. *Acta Meteor. Sinica*, **59**, 616–624. (in Chinese)
- , Zhang Limin, and Zhang Qinghong, 1994: The physical structure of the winter fog in Chongqing metropolitan area and its formation process. *Acta Meteor. Sinica*, **8**(3), 316–328.
- , Shi Chun'e, and Lu Taoshi, 1997: 3D model study on fog over complex terrain. Part II: Numerical experiment. *Acta Meteor. Sinica*, **11**, 88–94.
- , Huang Jianping, Huang Yusheng, et al., 1999: Study on the physical process of winter valley fog in Xishuangbanna region. *Acta Meteor. Sinica*, **13**(4), 494–508.
- Liu Duanyang, Pu Meijuan, Yang Jun, et al., 2010: Microphysical structure and evolution of a four-day persistent fog event in Nanjing in December 2006. *Acta Meteor. Sinica*, **24**, 104–115.
- , Yang Jun, Niu Shengjie, et al., 2011: On the evolution and structure of a radiation fog event in Nanjing. *Adv. Atmos. Sci.*, **28**, 223–237.
- Liu, Y. G., P. H. Daum, and R. McGraw, 2004: An analytical expression for predicting the critical radius in the autoconversion parameterization. *Geophys. Res. Lett.*, **31**, L06121.
- , —, and —, 2005: Size truncation effect, threshold behavior, and a new type of autoconversion parameterization. *Geophys. Res. Lett.*, **32**, L11811.
- , —, R. McGraw, et al., 2006: Generalized threshold function accounting for effect of relative dispersion on threshold behavior of autoconversion process. *Geophys. Res. Lett.*, **33**, L11804.
- , —, S. S. Yum, et al., 2008: Use of microphysical relationships to discern growth/decay mechanisms of cloud droplets with focus on Z-LWC relationships. Proc. 15th International Conference on Clouds and Precipitation, Cancun, Mexico, the International Commission on Clouds and Precipitation (ICCP).
- Lu, C. S., and S. J. Niu, 2008: Study on microphysical characteristics of winter fog in Nanjing area, China. Proc. 2008 International Workshop on Education Technology and Training & 2008 International Workshop on Geoscience and Remote Sensing, IEEE Computer Society, Shanghai, China, 273–276.
- , —, Yang Jun, et al., 2010a: Jump features and causes of macro and microphysical structures of a winter fog in Nanjing. *Chinese J. Atmos. Sci.*, **34**, 681–690. (in Chinese)
- , —, L. L. Tang, et al., 2010b: Chemical composition of fog water in Nanjing area of China and its related fog microphysics. *Atmos. Res.*, **97**, 47–69.
- , Y. G. Liu, and S. J. Niu, 2011: Examination of turbulent entrainment-mixing mechanisms using a combined approach. *J. Geophys. Res.*, **116**, D20207.
- Meyer, M. B., J. E. Jiusto, and G. G. Lala, 1980: Measurements of visual range and radiation-fog (haze) microphysics. *J. Atmos. Sci.*, **37**, 622–629.
- , G. G. Lala, and J. E. Jiusto, 1986: Fog-82: A cooperative field study of radiation fog. *Bull. Amer. Meteor. Soc.*, **67**, 825–832.
- Niu, F., Z. Q. Li, C. Li, et al., 2010a: Increase of wintertime fog in China: Potential impacts of weakening of the East Asian monsoon circulation and increasing aerosol loading. *J. Geophys. Res.*, **115**, D00K20.
- Niu, S. J., C. S. Lu, H. Y. Yu, et al., 2010b: Fog research in China: An overview. *Adv. Atmos. Sci.*, **27**, 639–661.
- , —, Y. G. Liu, et al., 2010c: Analysis of the microphysical structure of heavy fog using a droplet spectrometer: A case study. *Adv. Atmos. Sci.*, **27**, 1259–1275.
- , D. Y. Liu, L. J. Zhao, et al., 2012: Summary of a 4-year fog field study in northern Nanjing. Part 2: Fog microphysics. *Pure Appl. Geophys.*, **169**(5–6), 1137–1155.
- Petterssen, S., 1956: *Weather Analysis and Forecasting*. 2nd ed. Vol. 2, McGraw-Hill, 266 pp.

- Pilié, R. J., E. J. Mack, W. C. Kocmond, et al., 1975: The life cycle of valley fog. Part II: Fog microphysics. *J. Appl. Meteor.*, **14**, 364–374.
- Pinnick, R. G., D. L. Hoihjelle, G. Fernandez, et al., 1978: Vertical structure in atmospheric fog and haze and its effects on visible and infrared extinction. *J. Atmos. Sci.*, **35**, 2020–2032.
- Porson, A., J. Price, A. Lock, et al., 2011: Radiation fog. Part II: Large-eddy simulations in very stable conditions. *Bound.-Lay. Meteor.*, **139**, 193–224.
- Price, J., 2011: Radiation fog. Part I: Observations of stability and drop size distributions. *Bound.-Lay. Meteor.*, **139**, 167–191.
- Pu, M. J., G. Z. Zhang, W. L. Yan, et al., 2008: Features of a rare advection-radiation fog event. *Sci. China (Ser. D)*, **51**, 1044–1052.
- Quan, J., Q. Zhang, H. He, et al., 2011: Analysis of the formation of fog and haze in North China Plain (NCP). *Atmos. Chem. Phys.*, **11**, 8205–8214.
- Rémy, S., and T. Bergot, 2010: Ensemble Kalman Filter data assimilation in a 1D numerical model used for fog forecasting. *Mon. Wea. Rev.*, **138**, 1792–1810.
- Roach, W. T., 1976: On some quasi-periodic oscillations observed during a field investigation of radiation fog. *Quart. J. Roy. Meteor. Soc.*, **102**, 355–359.
- , R. Brown, S. J. Caughey, et al., 1976: The physics of radiation fog. I: A field study. *Quart. J. Roy. Meteor. Soc.*, **102**, 313–333.
- Rogers, R. R., and M. K. Yau, 1989: *A Short Course in Cloud Physics*. 3rd ed. Butterworth Heinemann, 290 pp.
- Roquelaure, S., and T. Bergot, 2008: A local ensemble prediction system for fog and low clouds: Construction, bayesian model averaging calibration, and validation. *J. Appl. Meteor. Climatol.*, **47**, 3072–3088.
- Shi Chun'e, Sun Xuejin, Yang Jun, et al., 1996: 3D model study on fog over complex terrain. Part I: Numerical study. *Acta Meteor. Sinica*, **10**, 493–506.
- , J. Yang, M. Y. Qiu, et al., 2010: Analysis of an extremely dense regional fog event in eastern China using a mesoscale model. *Atmos. Res.*, **95**, 428–440.
- , L. Wang, H. Zhang, et al., 2012: Fog simulations based on multi-model system: A feasibility study. *Pure Appl. Geophys.*, **169**(5–6), 941–960.
- Stoelinga, M. T., and T. T. Warner, 1999: Nonhydrostatic, mesobeta-scale model simulations of cloud ceiling and visibility for an east coast winter precipitation event. *J. Appl. Meteor.*, **38**, 385–404.
- Stolaki, S., I. Pytharoulis, and T. Karacostas, 2012: A study of fog characteristics using a coupled WRF-COBEL model over Thessaloniki airport, Greece. *Pure Appl. Geophys.*, **169**(5–6), 961–981.
- Tardif, R., and R. M. Rasmussen, 2007: Event-based climatology and typology of fog in the New York City region. *J. Appl. Meteor. Climatol.*, **46**, 1141–1168.
- Thalmann, E., R. Burkard, T. Wrzesinsky, et al., 2002: Ion fluxes from fog and rain to an agricultural and a forest ecosystem in Europe. *Atmos. Res.*, **64**, 147–158.
- Thoma, C., W. Schneider, M. Masbou, et al., 2012: Integration of local observations into the one dimensional fog model PAFOG. *Pure Appl. Geophys.*, **169**(5–6), 881–893.
- Tomasi, C., and F. Tampieri, 1976: Features of the proportionality coefficient in the relationship between visibility and liquid water content in haze and fog. *Atmosphere*, **14**, 61–76.
- Wang, G. L., L. M. Huang, S. X. Gao, et al., 2002: Characterization of water-soluble species of PM10 and PM2.5 aerosols in urban area in Nanjing, China. *Atmos. Environ.*, **36**, 1299–1307.
- , H. Wang, Y. J. Yu, et al., 2003: Chemical characterization of water-soluble components of PM10 and PM2.5 atmospheric aerosols in five locations of Nanjing, China. *Atmos. Environ.*, **37**, 2893–2902.
- Wang, J., P. H. Daum, S. S. Yum, et al., 2009: Observations of marine stratocumulus microphysics and implications for processes controlling droplet spectra: Results from the Marine Stratus/Stratocumulus Experiment. *J. Geophys. Res.*, **114**, D18210.
- Welch, R. M., M. G. Ravichandran, and S. K. Cox, 1986: Prediction of quasi-periodic oscillations in radiation fogs. Part I: Comparison of simple similarity approaches. *J. Atmos. Sci.*, **43**, 633–651.
- Wendisch, M., S. Mertes, J. Heintzenberg, et al., 1998: Drop size distribution and LWC in Po Valley fog. *Contrib. Atmos. Phys.*, **71**, 87–100.
- Wobrock, W., D. Schell, R. Maser, et al., 1992: Meteorological characteristics of the Po Valley fog. *Tellus B*, **44**, 469–488.
- Xue, Y., L.-P. Wang, and W. W. Grabowski, 2008: Growth of cloud droplets by turbulent collision-coalescence. *J. Atmos. Sci.*, **65**, 331–356.
- Yang, D., H. Ritchie, S. Desjardins, et al., 2010: High-resolution GEM-LAM application in marine fog prediction: Evaluation and diagnosis. *Wea. Forecasting*, **25**, 727–748.

- Yang, J., Y.-J. Xie, C.-E. Shi, et al., 2012: Ion composition of fog water and its relation to air pollutants during winter fog events in Nanjing, China. *Pure Appl. Geophys.*, **169**(5–6), 1037–1052.
- Yuan Jinnan and Huang Jian, 2011: An observational analysis and 3-dimensional numerical simulation of a sea fog event near the Pearl River Mouth in boreal spring. *Acta Meteor. Sinica*, **69**, 847–859. (in Chinese)
- Yue, Y. Y., S. J. Niu, L. J. Zhao, et al., 2012: Chemical composition of sea fog water along the South China Sea. *Pure Appl. Geophys.*, **169**, 2231–2249.
- , —, —, et al., 2013: Study on the synoptic system and macro-micro characteristics of sea fog along the Zhanjiang coastal area. *Chinese J. Atmos. Sci.*, **37**, 609–622. (in Chinese)
- Yum, S., 1998: Cloud droplet spectral broadening in warm clouds: An observational and model study. Ph. D. dissertation, University of Nevada, 191 pp.
- Zhang, S. P., 2012: Recent observations and modeling study about sea fog over the Yellow Sea and East China Sea. *Journal of Ocean University of China*, **11**, 465–472.
- Zhang Shuting, Niu Shengjie, and Zhao Lijuan, 2013: The microphysical structure of fog droplets in a sea fog event in the South China Sea. *Chinese J. Atmos. Sci.*, **37**, 552–562. (in Chinese)
- Zhang, Q., J. N. Quan, X. X. Tie, et al., 2011: Impact of aerosol particles on cloud formation: Aircraft measurements in China. *Atmos. Environ.*, **45**, 665–672.
- Zhao, L. J., S. J. Niu, Y. Zhang, et al., 2013: Microphysical characteristics of sea fog over the east coast of Leizhou Peninsula, China. *Adv. Atmos. Sci.*, **30**, 1154–1172.
- Zhou, B. B., and B. S. Ferrier, 2008: Asymptotic analysis of equilibrium in radiation fog. *J. Appl. Meteor. Climatol.*, **47**, 1704–1722.
- , and J. Du, 2010: Fog prediction from a multimodel mesoscale ensemble prediction system. *Wea. Forecasting*, **25**, 303–322.
- , J. Du, I. Gultepe, et al., 2012: Forecast of low visibility and fog from NCEP: Current status and efforts. *Pure Appl. Geophys.*, **169**(5–6), 895–909.
- Zhou, Y., S. J. Niu, and J. J. Lu, 2013: The influence of freezing drizzle on wire icing during freezing fog events. *Adv. Atmos. Sci.*, **30**, 1053–1069.